Characterizing Cultural Differences in Naturalistic Driving Interactions

Rachel DiPirro, Hauke Sandhaus, David Goedicke, Dan Calderone, Meeko Oishi, Wendy Ju

***Abstract*— The characterization of driver interactions is important for a variety of problems associated with the design of autonomy for vehicles. We consider the role of cultural context in driver interactions, by evaluating the differences in driving interactions in simulated driving experiments conducted in New York City, New York, USA, and in Haifa, Israel. The same experiment was conducted in both locations, and focused on naturalistic driving interactions at unsigned intersections, in which interaction with another vehicle was required for safe navigation through the intersection. We employ conditional distribution embeddings, a nonparametric machine learning technique, to empirically characterize differences in the distribution of trajectories that characterize driver interactions, across both locations. We show that cultural variability outweighs individual variability in intersections that require turning maneuvers, and that clear distinctions amongst driving strategies are evident between populations. Our approach facilities a data-driven analysis that is amenable to rigorous statistical testing, in a manner that minimizes filtering, pre-processing, and other manipulations that could inadvertently bias the data and obscure important findings.**

I. Introduction

The design of autonomy for vehicles requires reasoning not only about an individual vehicle's own actions, but also those of other vehicles that it interacts with. This requires the ability to infer and predict the other vehicle's likely actions [1], [2], [3], [4] in a manner that accommodates the ongoing feedback that occurs between vehicles as a maneuver proceeds. Driver interactions occur as a sequence of minute adjustments, communications, and actions by each driver. The dynamics of these interactions are difficult to model, in part because of the heterogeneiety amongst drivers, the social and cultural context, the driving scenario and driving context, and other human factors. For example, aggressive driving may be normalized in some communities, whereas defensive driving may be considered more appropriate in others [5], [6].

In a 1992 article in *Accident Analysis and Prevention,* David Zaidel posits the following possible mechanisms by which "others" can affect the behavior of individual drivers: others as a source of information, communication with others, others as a reference group, imitation of others [7]. Understanding the ways that drivers interact particularly in light of automation; as Oskar Juhlin presciently noted, "it is essential to understand how drivers themselves achieve coordination. Computers, running by rules or algorithms, must function together with other road users. [...] If the artificial drivers are socially incompetent, this could lead to ambiguity and misunderstandings which put serious strains on other road users" [8].

Currently, efforts to model and characterize the social interactions between cars have been based on data that models how single drivers respond to a computer-controlled vehicle [9], [10], [11] or models based on large scale naturalistic data [12], [13]; these approaches do not capture the communicative element which occurs between human-driven vehicles, nor the normativity wherein the driving patterns differ based on driving locale [14].

Our primary objectives in this paper are 1) to quantitatively characterize pairwise interactions between human-driven vehicles, and 2) to analyze how cultural context impacts these interactions. We seek to develop methodological approaches that enable high fidelity analysis of naturalistic driving interaction data. One major challenge to this type of analysis is the inherent heterogeneity of human driving data, especially under a naturalistic decision making context. We propose a data-driven approach, based in conditional distribution embeddings [15], that has been previously employed to characterize heterogeneity in driving trajectories [16], [17] and other human-in-the-loop systems [18]. We propose to use the maximum mean discrepancy, a metric in the reproducing kernel Hilbert space associated with the embedding [19], to quantitatively capture differences in distributions of driving data. This approach is responsive to the stochasticity inherent to trajectories of human-in-the-loop systems, and is particularly relevant for the extensive heterogeneity in driving interactions. Further, this approach requires little data processing or filtering that could inadvertently introduce bias or otherwise obscure phenomena of interest.

We are focused primarily in differences that occur in two cultural contexts: driving based in New York and in Israel. We employ data previously gathered from dyadic virtual reality driving simulator experiments conducted both in New York City, USA and Haifa, Israel. The two sites of data collection, New York and Israel, were based on the location of the Goedicke et al.'s collaborative research teams [20]. This "place-based" proxy for culture represents only a limited part of the beliefs, values, norms, and things people use to guide their social interactions in everyday life [21], but was intended to capture at least how people from different places behave, presumably based on differences in driving norms. These studies are first-of-their-kind dyadic studies

This material is based upon work supported by the National Science Foundation under NSF Grants No. 2227338 and 2107111. Any opinions, findings, and conclusions or recommendations expressed in this material are those of the authors and do not necessarily reflect the views of the National Science Foundation.

Rachel DiPirro, Dan Calderone, and M. Oishi are with Electrical & Comp. Eng., Univ. of New Mexico, Abq., NM. Hauke Sandhaus, David Goedicke, and Wendy Ju are with Information Science, Cornell Tech, New York, NY 10044. Email: {rdipirro,dcalderone,oishi}@unm.edu, {hgs52,dg536,wendyju}@cornell.edu.

involving naturalistic driving behaviors, albeit captured in simulation to control the environment and scenarios; this data captures the dynamics of how people move their vehicles to take lead or yield in driving encounters, sometime cycling between both in response to the other.

The paper is organized as follows. Section II describes the cross-cultural human subjects experiment. Section III describes the treatment of the data and application of the maximum mean discrepancy metric. Section IV presents the main results in identifying differences between driver populations. Section V concludes the paper.

II. Experimental Setup

A. Participants

This study was conducted under Cornell University's Institutional Review Board approval in New York City (IRB0008479) and under Technion's Ethics Committee Request in Israel. We recruited at both locations through flyers, word of mouth, and mailing lists. The study included a total of 170 participants, in 85 dyads: 42 in Israel and 43 in New York. Due to motion sickness, 9 dyads were stopped prematurely and were excluded from analysis (5 from Israel and 4 from New York). The majority of participants were between the ages of 18 and 34 (85%) and the proportion of females to males was nearly equal (46% and 54%, respectively). A total of 97% of the participants had driver's licenses, 28% for less than 5 years, and 45% for 5–10 years. A total of 33% of the driving participants reported driving 1–2 days per week on average, and 23% of participants reported driving 3–4 days a week. A total of 80% of the participants had not driven outside of their own country. Most participants reported a lack of experience in virtual reality games (18% never played; 38% were novices). Most participants (42%) did not report any motion sickness during virtual reality games. Since the study was conducted in pairs, the participants were asked about their acquaintance with their partner; 47% of participants reported no acquaintanceship.

B. Experimental testbed

For scenario deployment and data gathering, we used the open-source StrangeLand driving simulator [20], which enables multi-participant driving interaction. This simulator records vehicle motion, such as wheel and steering wheel motion, indicator lights, driver position, and hand gestures for both participants' cars. Additional tools were added to support the recording and post-facto replay of the entire study. The study used Quest 2 virtual reality headsets and Logitech steering wheels mounted to tables. To mitigate simulator sickness, measures such as room ventilation, a pleasant odor, and ginger candies were prepared [22].

The simulator was situated in a research laboratory. Participants sat next to one another, unaware that they were in the same virtual environment (Figure 1). Each driver observed partial representations (captured by the virtual reality headset hand and head tracking) of themselves in the virtual environment, including a reflection of their avatar face in the mirror and their hands on the steering wheel (Figure 2). Each could also see the other driver in the other vehicle when they encountered one another in the scenarios.

Fig. 1. The experiment was conducted in virtual driving simulators in two locations: Haifa, Israel and New York City, New York. Two participants, seated next to each other, had multiple driving interactions with each other in the same StrangeLand driving environment [20].

Fig. 2. Each participant's view within the virtual environment provides a realistic driving view that consists of the dashboard of their own vehicle, their hand movements projected within the virtual environment, the simulated external environment, and the car of the other driver. The green arrow instructs the participant of the next maneuver.

C. Study design

Seven intersection traffic scenarios involving ambiguous right-of-way were developed. We used crash scenario ranking statistics (crash frequency, economic cost, and functional years lost) [23], [24] for multi-vehicle incidents to select these scenarios. These scenarios were designed to require participants to communicate and negotiate with one another with their virtual cars to complete their driving tasks.

The participants were able to drive freely within the simulator; to coordinate the interaction of the participants, the intersection scenarios were controlled by traffic control, such as traffic lights located a block before the intersection for each participant, which turned green at the same time [25]. While we considered other viable methods to increase the likelihood of encounters, such as dynamically modified speed adjustment [26], [25] and dynamic route length change, these were not ultimately used in our study.

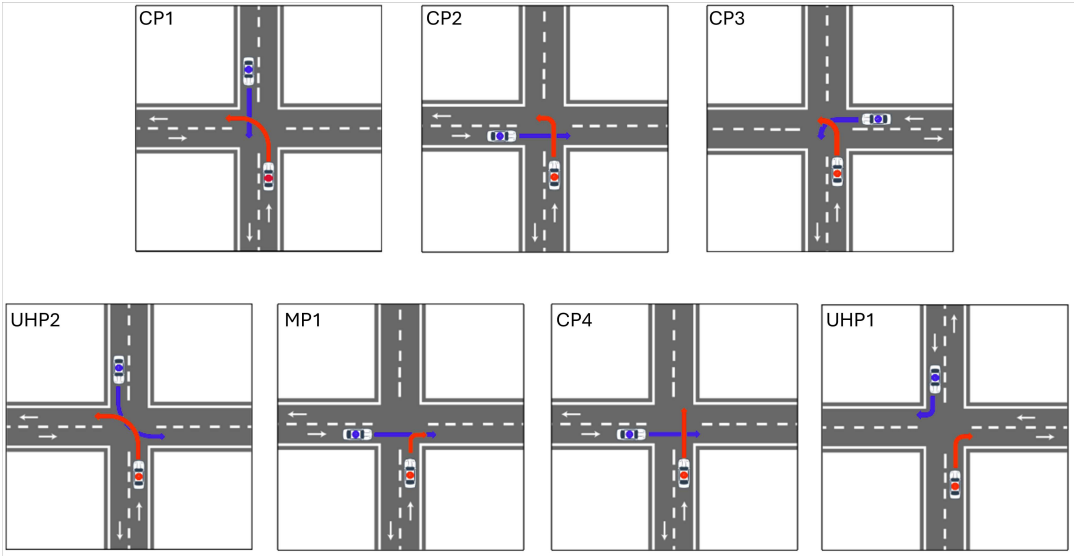

Fig. 3. A total of seven driving scenarios were analyzed. Car A is denoted in red and Car B is denoted in blue. As in [14], the scenarios are abbreviated by 'CP,' which indicates Crossing Paths, 'UHP,' which indicates Unconstrained Head-On Paths, and 'MP,' which indicates Merging Paths.

D. Experimental procedure

Participants were informed about the risk of simulator sickness and consent was obtained. Participants were next instructed on how to put on the virtual reality headset, and they entered the virtual world and drove for approximately 40 minutes in 12 different driving scenarios. The driving instructions were displayed on the vehicle's dashboard through arrows (Figure 2), and each participant drove the vehicle as instructed using the steering wheel and gas and brake pedals. Drivers drove across a curvy road section, to familiarize themselves with how the vehicle maneuvered in the virtual world. They stopped at a red traffic light and drove into the intersection at the same time. After they negotiated right-of-way and passed the intersection, the scenario ended at a do not enter sign. The order of scenarios was randomized for each pair of participants using a Latin Square design.

E. Data gathering

Experimental data from the simulator was gathered at approximately 18 frames per second, and included car location, velocity, acceleration, and heading. Experimental data from the human was also gathered at the same frame rate, and included steering angle, gas pedal and brake pedal, hand position and orientation, and head position and orientation.

Videos of the data used in this analysis are available at the Cross Cultural Driver Interaction Data OSF project repository (https://osf.io/bz8vq/) [27].

III. Methods

A. Data selection and pre-processing

1) Automated identification of interaction scenarios: We wish to only consider data from scenarios in which participants experience an interaction, and hence need to exclude data that does not reflect actual interaction. However, identifying interactions manually is challenging because it relies upon qualitative assessments that often require subjective human judgement. For example, the definition in [14] describes a driving interaction as a situation where the behavior of at least two road users is influenced by the possibility of occupying the same space in the near future.

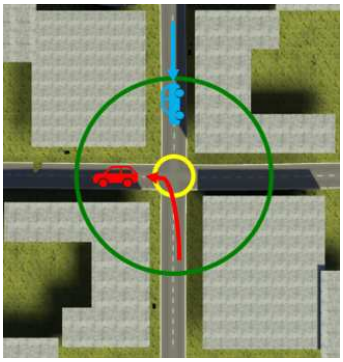

Fig. 4. A driving interaction is presumed to occur when both vehicles are simultaneously within a circle of radius 25 meters (green). The trajectory associated with the driving interaction begins once both vehicles enter the circle, and ends when one car leaves the intersection, as captured via a circle centered at the intersection (yellow), with radius 5 meters.

We propose an automated process for binary classification of all of the driving scenarios in Figure 3, as either depicting an interaction, or not, to replace the subjective and time-intensive task of manually labelling whether an interaction between drivers has transpired. We use criteria based on vehicle proximity to the intersection. Specifically, a driving interaction is presumed to occur when both vehicles are simultaneously within a circle of radius 25 meters (Figure 4), and at least one vehicle is in front of the other vehicle.

We validated this approach through analysis of a sampled subset of all scenarios. We considered a random selection of 10 samples of each of the seven scenarios in Figure 3. For each scenario in this selection, we carefully examined the

TABLE I

AUTOMATED CLASSIFICATION OF TRAJECTORIES WHICH DEPICT INTERACTIONS

	Interaction Predicted	**No Interaction Predicted**
Interaction Observed	100 (76%)	2 (1%)
No Interaction Observed	9 (7%)	21 (16%)

scenario using a virtual reality study replay tool [28] which enabled re-enactment of the scenario. The accuracy of our automated rule-based classifier as compared to this manual classification is shown in Table I. Overall, our method had 92% accuracy. Misclassifications were primarily due to differing nominal speeds between Car A and Car B.

Based on these criteria, a total of 380 trajectories from the seven scenarios in Figure 3 were included in our analysis, with 211 from Israel and 169 from New York. A total of 57 trajectories were excluded from the analysis, due to their classification of no interaction between the two drivers.

2) Trajectory pre-processing: After identifying scenarios via our automated classifier, we then considered how to methodologically isolate trajectories from each scenario.

Each trajectory consists of vectors of driving relevant data, from both cars (Car A and Car B), recorded over a finite time horizon. We consider multiple combinations of data from which to construct trajectories:

1) *Path:* Car positions, in planar coordinates.
2) *Path + Acceleration + Steering Angle:* Car positions, in planar coordinates; accelerations, in planar coordinates; steering angles.
3) *Steering:* Steering angles.

These combinations have been selected because they emphasize factors that overtly reflect interaction amongst the two cars. Inclusion of path data enables analysis of spatial differences in maneuvers such as turning. Inclusion of inputs (acceleration and steering) enables analysis of elements closer to the driver's intent; these could elucidate differences in driving style. Lastly, we include steering in isolation because it reflects immediate changes in maneuvers. For the *Path + Acceleration + Steering Angle* data combination, we normalized each element to be of comparable values.

For each data combination, we then isolate trajectories within each scenario that have been deemed to demonstrate driver interactions. The goal of this isolation is to capture just the parts of the trajectories that could be impacted by interactions. Excision of the trajectories from the larger data set requires a methodological approach to avoid accidentally biasing the analysis. We choose the start time for the trajectory as the first time step at which both vehicles are within the 25 meter radius circle located at the center of the intersection. The end time for the trajectory occurs when the first vehicle leaves the intersection, which is defined through a circle with a radius of 5 meters, also co-located with the center of the intersection (Figure 4).

Lastly, we normalize the length of all trajectories for a given scenario by re-sampling, so that all trajectories for a given scenario are of the same length. The re-sampling is required to facilitate analysis via conditional distribution embeddings. We ensure validity in creation of and comparison of distributions by ensuring that all trajectories are projected into the same reproducing kernel Hilbert space. We choose the re-sampled trajectory length to be 200 time steps, the average length of the trajectories before sampling. The resampling factor ranges between 0.06 and 3.50 for all trajectories considered here.

TABLE II

NUMBER OF TRAJECTORIES IN EACH DISTRIBUTION, CATEGORIZED BY SCENARIO, LOCATION, AND LEAD CAR

Scenario	**NYC, Lead Car A**	**NYC, Lead Car B**	**Israel, Lead Car A**	**Israel, Lead Car B**
CP1	12	13	10	20
CP2	11	11	15	15
CP3	13	11	9	25
UHP1	16	9	12	16
CP4	11	14	23	10
MP1	15	10	13	14
UHP2	8	15	15	16

3) Creating distributions of trajectories: Once the trajectories are pre-processed, we group the trajectories by a) scenario, and b) the first car to arrive at an intersection, referred to as the "lead car", as we observe that this significantly impacts the behavior of the drivers. For instance, in scenario CP1 (Figure 3), if Car A (red) arrives first, the vast majority of the turn executed by Car A is captured in the trajectory. However, if Car B arrives first, the trajectory ends before Car A is able to execute a turn, as Car B clears the intersection before Car A completes their turn. Separating trajectories according to the first car to arrive avoids confounding factors that could obscure evidence of site-specific driving traits.

By considering combinations of scenario and first car to arrive, we obtain a total of 28 distributions of trajectories. That is, for each of the seven scenarios, at each of two sites, we separately consider the case in which Car A arrives first, and the case in which Car B arrives first. The number of trajectories in each distribution is described in Table II.

B. Distance metrics between distributions of trajectories

Consider a trajectory that is described via a stochastic process [29], $X = \left[\mathbf{x}_1^T, \mathbf{x}_2^T, \cdots, \mathbf{x}_N^T\right]^T \in \mathbb{R}^{mN}$, over a horizon of length N time steps. For an interacting pair of vehicles, we presume that the stochastic process at time step t is described by $\mathbf{x}_t = \left[x_t^A, x_t^B\right] \in \mathbb{R}^m$, where x_t^A, x_t^B correspond to the data recorded for Car A and Car B, respectively, as described in Section III-A. This formalism arises from viewing the trajectory as resulting from the evolution of a discrete-time, stochastic, dynamical system.

We presume that the distribution $\mathbb{P}$ of X is unknown, but that we have access to samples $\mathcal{S} = \{\xi^i\}_{i=1}^M$, $\xi^i \in \Xi \subseteq \mathbb{R}^{mN}$, drawn independently and identically from $\mathbb{P}$. We seek to first empirically represent the distribution $\mathbb{P}$ via its samples $\mathcal{S}$, where each sample corresponds to a trajectory from one of

the 28 distributions we have identified, and then to compute the distance between two relevant distributions, $\mathbb{P}$ and $\mathbb{Q}$.

To do so, we employ a non-parametric learning method, conditional distribution embeddings [30], which finds the best fit conditional distribution amongst a set of distributions in a reproducing kernel Hilbert space $\mathscr{H}$ (RKHS), which is a linear space of functions of the form $f : \mathcal{X} \to \mathbb{R}$ equipped with the inner product $\langle \cdot, \cdot \rangle_{\mathscr{H}}$. This requires two weak assumptions: 1) x is continuous, and b) $\mathbb{P}$ is smooth. Observed data is projected into a Hilbert space defined by a positive semi-definite kernel function $k : \mathcal{X} \times \mathcal{X} \to \mathbb{R}$, that captures the pairwise "distance" between any two data points. A regularized least squares problem then fits the conditional distribution in the Hilbert space to observed data.

We chose the radial basis kernel, $k(\xi, \xi') = \exp(-\|\xi - \xi'\|^2/2\sigma^2)$ because we have previously found it to be effective for human-in-the-loop data [16], [17]. We choose $\sigma = 13$ for *Path data*, $\sigma = 1$ for *Path + Acceleration + Steering Angle*, and $\sigma = 2$ for *Steering Angle*, chosen for each dataset via grid search. The kernel distribution embedding of $\mathbb{P}$ [30], $m_{\mathbb{P}} = \int_{\Xi} k(\xi, \cdot)\mathbb{P}(\mathrm{d}\xi)$, captures the distribution $\mathbb{P}$ within the RKHS, and is empirically approximated as $\widehat{m}_{\mathbb{P}} = \frac{1}{M}\sum_{i=1}^{M} k(\xi^i, \cdot)$.

We can calculate the distance between two distributions via the the maximum mean discrepancy (MMD) [31], a norm in the Hilbert space, defined as $\mathrm{MMD}(\mathbb{P}, \mathbb{Q}) = \|m_{\mathbb{P}} - m_{\mathbb{Q}}\|^2_{\mathscr{H}}$. The MMD is empirically approximated as

$$\widehat{\mathrm{MMD}}(\mathbb{P}, \mathbb{Q}) = \left\| \frac{1}{M}\sum_{i=1}^{M} k(\xi^i, \cdot) - \frac{1}{N}\sum_{i=1}^{N} k(\xi^i, \cdot) \right\|^2_{\mathscr{H}}. \quad (1)$$

Although multiple metrics to capture distance between distributions exist, such as the Kullback-Leibler divergence or total variation divergence, many require density estimation, which can be computationally expensive and numerically unstable. Additionally, we have found in our previous work that MMD is responsive to the underlying characteristics of the distribution [16], [17].

For each scenario, we use the MMD to compare the distribution $\mathbb{P}$ for a given site and first car to arrive to a baseline trajectory, represented as the distribution $\mathbb{Q}$. The baseline trajectory for each scenario and first-to-arrive car is computed via successive convex programming [32], by optimizing costs that penalize constraint violation, subject to vehicle dynamics. We employ the same baseline trajectory for each scenario and first-to-arrive car, across both sites. That is, we compute the MMD between the distribution from the New York site and the baseline trajectory, and from the distribution from the Israel site and the baseline trajectory, separately for both Car A arriving first and Car B arriving first. By employing the MMD with respect to the baseline trajectory, we can evaluate the relative distance of each distribution from a neutral trajectory.

To compute the baseline trajectories, we presume the vehicle dynamics can be represented simply through a unicycle model with state vector $[x, z, v, \phi]$ with linear velocity v and heading angle ϕ [33]. We presume the control inputs are linear acceleration a and angular velocity ω. The continuous time unicycle dynamics,

$$\dot{x} = v\cos\phi, \quad \dot{z} = v\sin\phi, \quad \dot{v} = a, \quad \dot{\phi} = \omega$$

are discretized via a forward-Euler integration scheme. The initial and terminal states in the optimization are chosen to match the average value taken from all trajectories for each scenario. The cost function weights acceleration inputs with a value of 1 and the angular velocities with a value of 10. For each turning maneuver, we define keep out regions as shown in Figure 5, rotated as appropriate for the starting direction of each the turning car, with a penalty weight of 10^4.

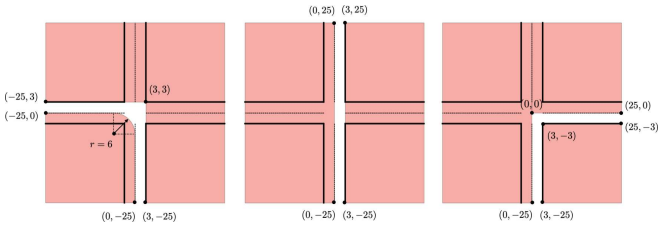

Fig. 5. Keep out regions for construction of baseline trajectories for left turn, straight, and right turn.

We employ the known relationship between the heading angle of the unicycle model and the steering angle of the more complex bicycle model of vehicle dynamics via $\omega = \frac{v}{\ell}\tan\psi$ [34], where ℓ is the distance between the axles of the bicycle (which we presume to be $\ell = 2.5$ meters), to obtain baseline trajectories in steering angle.

IV. Results

One of the unique features of this project is that we can establish the casual relationship between the drivers' goals and their interactions, which is not present in models based on large-scale naturalistic data. The other is that, because we have run the study between two distinct sites, we can better distinguish between aspects of interactions which are inherent to the scenario, and aspects which are normative– things that drivers do based on the shared understanding of what other drivers will expect; this is not possible in analyses of interaction based on single participant behavior. We attempted to minimize variations in experimental setup and participant experience between the two sites but cannot entirely rule out that observed differences could be caused by factors other than cultural norms.

This analysis was performed using the SOCKS toolbox [35] in Python.

A. Differences across sites are evident via MMD

Main Finding #1: *It is possible to quantify driving differences between sites using MMD as a metric.*

Differences between distributions are evident in the magnitude of the MMD, compared for each scenario and lead car between the two sites (Figure 6). That is, comparing the red solid and red unshaded bars, and comparing the blue solid and blue unshaded bars, shows distinct differences in almost

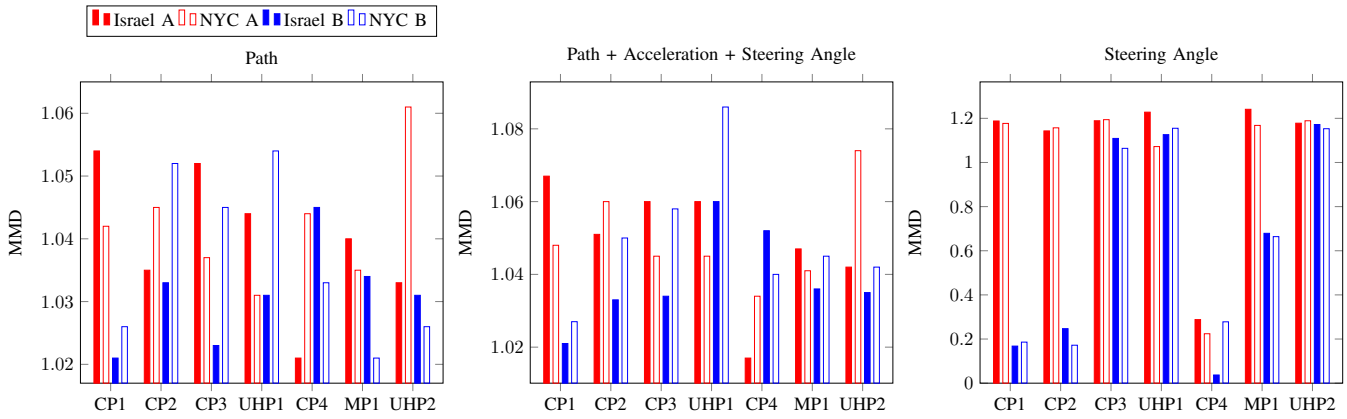

Fig. 6. Differences in MMD values between sites support the hypothesis that differences in driving interactions can be identified via the MMD metric. This finding is consistent across all combinations of data selection.

all cases. This result is consistent across all combinations of data, as shown in Figure 6.

The raw value of the MMD is determined primarily by the baseline trajectory, and its relationship to the two distributions (NYC and Israel), for a given lead car. We are focused primarily on the relative differences between MMD values, because it indicates the relative differences between distributions, with respect to the baseline trajectory. To validate these findings, we employ a leave-one-out-analysis. We focus on scenarios CP1, CP3, CP4, and MP1, which inform the remainder of our main findings. For each scenario, we remove one trajectory from the distribution and re-compute the MMD. Table III shows that differences between MMD values persist, demonstrating robustness to potential outliers.

We conducted a permutation statistical test (Table IV) with the MMD as a test statistic. A random number of trajectories were swapped between the NYC and Israel distributions for both Lead Car A and B, and the MMD was recalculated. We repeated this process 1,000 times for each distribution, and calculated the probability that the MMD between the permuted distributions was at least as large as its original value. No statistical significance was found in most cases, for several reasons: First, the number of samples in each distribution is relatively small (between 8 and 25 trajectories), which could easily confound tests for statistical significance. Second, the nature of the MMD is that it provides distance, but not direction. Because we calculate the MMD with respect to a baseline distribution, it possible there are important differences in the distributions, despite similar MMD values. Indeed, calculating the MMD between two distributions directly (as opposed to the MMD between a distribution and the baseline), as in Table V, shows that the populations show distinct differences.

B. Specific driving maneuvers differ between sites.

By determining prominent differences in MMD across sites, we can identify maneuvers that vary between sites.

Main Finding #2: *Acceleration and deceleration maneuvers differ between sites.*

TABLE III

MEAN ± STANDARD DEVIATION OF MMD LEAVE-ONE-OUT ANALYSIS

Scenario	NYC, Lead Car A	NYC, Lead Car B	Israel, Lead Car A	Israel, Lead Car B
CP1 *Path*	1.093 ± 0.001	1.059 ± 0.004	1.125 ± 1.065e−5	1.046 ± 0.002
CP3 *Path*	1.083 ± 4.304e−3	1.101 ± 0.001	1.121 ± 0.002	1.047 ± 0.001
CP4 *Path*	1.100 ± 3.093e−4	1.073 ± 0.001	1.044 ± 9.681e−4	1.102 ± 0.003
CP4 *Steering Angle*	0.052 ± 0.005	0.079 ± 0.005	0.084 ± 0.006	0.142 ± 0.017
MP1 *Path*	1.075 ± 0.001	1.053 ± 0.017	1.088 ± 0.001	1.074 ± 0.002

Acceleration as a maneuver with differences between sites is evident in scenario MP1 (Figure 6), in which the *Path* MMD for NYC participants is smaller than the *Path* MMD for Israel participants, regardless of which car arrives first. The higher MMD values indicate that the Israel distribution is farther from the baseline than NYC distribution. The higher *Path* MMD for both Israel distributions suggests that the positional difference is due to how the cars approach the intersection, implying that there is a difference in the speed and therefore acceleration and deceleration tendencies between the sites. The *Path* data (Figure 7) demonstrates differences in acceleration between the sites using the average acceleration values for each of the distributions. On average, we see that for the Lead Car A distributions, the Israel distribution (Figure 7, lower left) accelerates more slowly through the turn than the NYC Lead Car A distribution average (upper right). For the Lead Car B distributions, we can observe differences in the braking behavior: the Israel Lead Car B distribution average (lower right) brakes for less time than the NYC Lead Car B distribution average, presumably because they are traveling more slowly as they approach the intersection.

Main Finding #3: *Turning maneuvers differ between sites.*

In multiple scenarios, maneuvers involving turning showed differences in MMD values across sites. Consider scenario

TABLE IV

P-VALUES FOR EACH DISTRIBUTION FROM PERMUTATION TEST

Scenario	NYC, Lead Car A	NYC, Lead Car B	Israel, Lead Car A	Israel, Lead Car B
CP1 *Path*	0.021	0.788	0.859	0.107
CP3 *Path*	0.354	0.775	0.772	0.103
CP4 *Path*	0.284	0.818	0.129	0.077
CP4 *Steering Angle*	0.903	0.833	0.095	0.229
MP1 *Path*	0.465	0.395	0.529	0.793

TABLE V

MMD VALUES BETWEEN NYC AND ISRAEL DISTRIBUTIONS

Scenario	Lead Car A	Lead Car B
CP1 *Path*	0.443	0.360
CP3 *Path*	0.430	0.362
CP4 *Path*	0.386	0.414
CP4 *Steering Angle*	0.209	0.218
MP1 *Path*	0.366	0.405

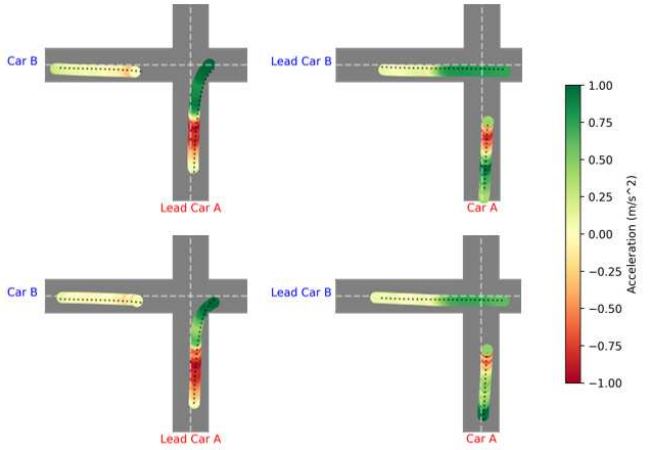

Fig. 7. Average acceleration data in scenario MP1 shows differences across sites. The NYC distributions (top) show faster acceleration in the Lead Car A distribution (left) and more braking in the Lead Car B distribution (right) than their Israel counterparts (bottom).

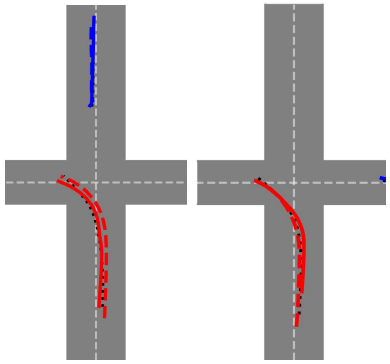

Fig. 8. Average trajectories in scenarios CP1 (left) and CP3 (right) show differences between the sites. In both scenarios, the mean trajectory of the Israel Lead Car A distribution (solid red) deviates from the baseline trajectory (black dotted), turning more sharply than the mean trajectory of NYC Lead Car A distribution (dashed red).

CP1, where the difference in MMD values between which car leads is greater than the differences in MMD values between the sites for the *Path* data in Figure 6. This is due to the fact that when Car A, the car prescribed to turn in this scenario, arrives at the intersection first, the entire turn is captured within the trajectory. When Car B arrives at the intersection first, it leaves the intersection and hence the trajectory ends before the turning car completes their turn. This difference highlights that the turn is a significant maneuver when considering the differences between the sites.

In scenario CP1, with Lead Car A, the Israel site distribution shows a higher MMD value than the NYC site, indicating a larger distance from the baseline (Figure 6). While the mean trajectory of the Israel site and NYC site distributions (Figure 8) are similar to the baseline trajectory, the average path for the Israel distribution deviates more from the baseline trajectory than NYC, which is reflected in a higher MMD values for the Israel Lead Car A distribution. A similar trend exists in scenario CP3, which also shows higher MMD values for Lead Car A trajectories for the Israel site than for the NYC site. In scenario CP3, in which Car A is making a left turn, drivers at the Israel site deviate more from the baseline than drivers at the NYC site (Figure 8). The deviation takes the form of a sharper turn shape in the Israel distribution than the NYC distribution. We hypothesize this is due to differences in traffic laws: In Israel, left turns are only performed when oncoming traffic is stopped, whereas unprotected left turns are common in New York City.

C. Comparing relative changes in MMD across data combinations can illuminate differences in the data.

Main Finding #4: *Changes in steering angle do not significantly impact path.*

Subtle differences can be identified between sites when comparing the relative trends across data types. We focus specifically on *Steering* and *Path* data. Consider the trends between MMD values across sites in scenario CP4 (Figure 6, left), with *Path* data: for Lead Car A, the NYC site has a higher MMD value than the Israel site. However, for MMD values based in *Steering* data for CP4 (Figure 6, right), we observe the opposite: the NYC site has a *lower* MMD value than the Israel site. We believe that this indicates that the Israel site drivers perform steering maneuvers that are not necessarily captured in *Path* data. We hypothesize that manipulation of the steering wheel at lower speeds, when the steering input will not have much impact on the vehicle trajectory, will not be reflected in the *Path* data.

Figure 9 shows the differences in the steering angle between sites for scenario CP4 using the averages of the distributions. When Car A arrives at the intersection first, the Israel distribution has the higher MMD value for *Steering* data, but the lower MMD value for *Path*, indicating that although the Israel Lead Car A average trajectory takes an expected path through the intersection, the steering inputs to achieve this path are different than the baseline. This is reflected in the positive steering angle for Lead Car A as it crosses the intersection (shown in green), as the baseline trajectory uses a primarily negative steering angle within the

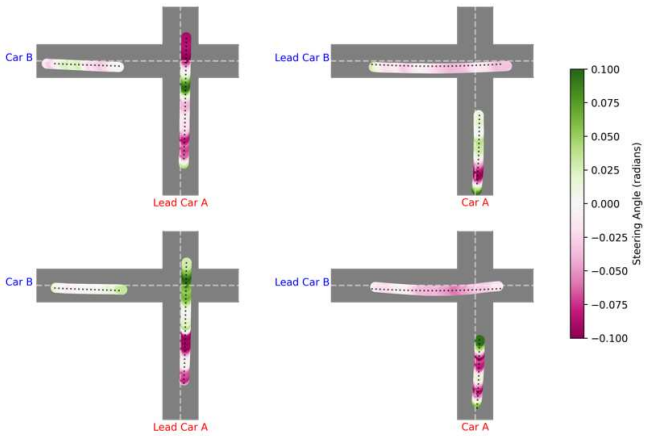

Fig. 9. The averages of the steering angle for scenario CP4, for NYC distributions (top), and Israel distributions (bottom).

intersection. On the other hand, when Car B arrives at the intersection first, the NYC distribution has a higher *Steering* MMD value, but a lower *Path* MMD value than the Israel distribution, suggesting that the NYC Lead Car B steering distribution deviates more from the baseline in this case.

V. Conclusion

We employ kernel distribution embeddings to characterize differences between populations of drivers in naturalistic driving interaction scenarios. Specifically, we use MMD to identify granular differences that may be missed by prototypical statistical methods. Understanding the impacts of interactions between drivers is important for future design of culturally aware autonomous vehicles.

References

[1] D. Sadigh, K. Driggs-Campbell, A. Puggelli, W. Li, V. Shia, R. Bajcsy, A. Sangiovanni-Vincentelli, S. Sastry, and S. Seshia, "Data-driven probabilistic modeling and verification of human driver behavior," in *AAAI Spring Symp-Tech Rep*, 2014, pp. 56–61.

[2] A. Narang, E. Faulkner, D. Drusvyatskiy, M. Fazel, and L. Ratliff, "Multiplayer performative prediction: Learning in decision-dependent games," *Jrnl Mach. Learning Res.*, vol. 24, no. 202, pp. 1–56, 2023.

[3] C. Fox, F. Camara, G. Markkula, R. Romano, R. Madigan, and N. Merat, "When should the chicken cross the road?-game theory for autonomous vehicle-human interactions," in *Proc Int'l Conf Vehicle Technology & Intel Transp Sys*. SciTePress, 2018, pp. 431–439.

[4] S. Amsalu and A. Homaifar, "Driver behavior modeling near intersections using hidden markov model based on genetic algorithm," in *IEEE Int'l Conf Intel Transp Eng*, 2016, pp. 193–200.

[5] P. Hancock, "Some pitfalls in the promises of automated and autonomous vehicles," *Ergonomics*, vol. 62, no. 4, pp. 479–495, 2019.

[6] T. Özkan, T. Lajunen, J. E. Chliaoutakis, D. Parker, and H. Summala, "Cross-cultural differences in driving behaviours: A comparison of six countries," *Transportation research part F: Traffic psychology and behaviour*, vol. 9, no. 3, pp. 227–242, 2006.

[7] D. Zaidel, "A modeling perspective on the culture of driving," *Accident Analysis & Prevention*, vol. 24, no. 6, pp. 585–597, 1992.

[8] O. Juhlin, "Traffic behaviour as social interaction-implications for the design of artificial drivers," in *World Congr Intel Transp Sys*, 1999.

[9] D. Sadigh, S. Sastry, S. Seshia, and A. Dragan, "Planning for autonomous cars that leverage effects on human actions," in *Robotics: Science and Systems*, vol. 2, 2016, pp. 1–9.

[10] D. Sadigh, N. Landolfi, S. Sastry, S. Seshia, and A. Dragan, "Planning for cars that coordinate with people: Leveraging effects on human actions for planning and active information gathering over human internal state," *Autonomous Robots*, vol. 42, pp. 1405–1426, 2018.

[11] X. Zhao, J. Sun, and M. Wang, "Measuring sociality in driving interaction," *IEEE Trans Intel Transp Sys*, pp. 1–14, 2024.

[12] A. Kuefler, J. Morton, T. Wheeler, and M. Kochenderfer, "Imitating driver behavior with generative adversarial networks," in *IEEE Intel Vehicles Symp*, 2017, pp. 204–211.

[13] K. Driggs-Campbell, V. Govindarajan, and R. Bajcsy, "Integrating intuitive driver models in autonomous planning for interactive maneuvers," *IEEE Trans Intel Transp Sys*, vol. 18, no. 12, pp. 3461–3472, 2017.

[14] G. Markkula, R. Madigan, D. Nathanael, E. Portouli, Y. M. Lee, A. Dietrich, J. Billington, A. Schieben, and N. Merat, "Defining interactions: A conceptual framework for understanding interactive behaviour in human and automated road traffic," *Theoretical Issues in Ergonomics Science*, vol. 21, no. 6, pp. 728–752, 2020.

[15] L. Song, J. Huang, A. Smola, and K. Fukumizu, "Hilbert space embeddings of conditional distributions with applications to dynamical systems," in *Proc. Int'l Conf. Machine Learning*, 2009, p. 961–968.

[16] K. Ortiz, A. J. Thorpe, A. Perez, M. Luster, B. Pitts, and M. Oishi, "Characterizing within-driver variability in driving dynamics during obstacle avoidance maneuvers," *IFAC Workshop Cyber-Physical Human Syst*, vol. 55, no. 41, pp. 13–19, 2022.

[17] H. Sridhar, G. Huang, A. Thorpe, M. Oishi, and B. Pitts, "Characterizing the effect of mind wandering on braking dynamics in partially autonomous vehicles," *ACM Trans Cyber-Physical Sys*, 2024.

[18] M. S.-T. Yuh, K. R. Ortiz, K. S. Sommer-Kohrt, M. Oishi, and N. Jain, "Classification of human learning stages via kernel distribution embeddings," *IEEE Open Jrnl Control Sys*, vol. 3, pp. 102–117, 2024.

[19] Y. Nemmour, H. Kremer, B. Schölkopf, and J.-J. Zhu, "Maximum mean discrepancy distributionally robust nonlinear chance-constrained optimization with finite-sample guarantee," in *Proc IEEE Conf. Dec. Control*, 2022, pp. 5660–5667.

[20] D. Goedicke, C. Zolkov, N. Friedman, T. Wise, A. Parush, and W. Ju, "Strangers in a Strange Land: New Experimental System for Understanding Driving Culture Using VR," *IEEE Trans Vehicular Technology*, vol. 71, no. 4, p. 3399–3413, Apr. 2022.

[21] J. Moeckli and J. Lee, "The making of driving cultures," *Improving Traffic Safety Culture in the US*, vol. 38, no. 2, pp. 185–192, 2007.

[22] S. Rangelova and E. Andre, "A survey on simulation sickness in driving applications with virtual reality head-mounted displays," *Presence: Teleoperators and Virtual Env.*, vol. 27, no. 1, pp. 15–31, Feb. 2018.

[23] W. Najm and D. Smith, "Definition of a pre-crash scenario typology for vehicle safety research," in *Proc. Int'l Tech Conf Enhanced Safety Vehicles*, 2007, p. 10.

[24] K. Czarnecki, "Operational world model ontology for automated driving systems–part 2: Road users, animals, other obstacles, and environmental conditions," Univ of Waterloo, Tech. Rep., 2018.

[25] J. Schindler and F. Köster, "A dynamic and model-based approach for performing successful multi-driver studies," *Proc DSC Europe*, 2016.

[26] P. Hancock and S. De Ridder, "Behavioural accident avoidance science: Understanding response in collision incipient conditions," *Ergonomics*, vol. 46, no. 12, pp. 1111–1135, Oct. 2003.

[27] H. Sandhaus, R. DiPirro, D. Goedicke, N. Klein, M. Oishi, A. Parush, and W. Ju, "Cross cultural driver driver interaction data," Aug 2024. [Online]. Available: osf.io/bz8vq

[28] D. Goedicke, H. Haraldsson, N. Klein, L. Zhou, A. Parush, and W. Ju, "ReRun: Enabling multi-perspective analysis of driving interaction in VR," in *ACM/IEEE Int'l Conf Human-Robot Int*, 2023, p. 889–890.

[29] E. Cinlar, *Probability and Stochastics*. Springer, 2011.

[30] A. Smola, A. Gretton, L. Song, and B. Schölkopf, "A Hilbert space embedding for distributions," in *Algorithmic Learning Theory*. Springer, 2007, pp. 13–31.

[31] A. Gretton, K. Borgwardt, M. Rasch, B. Schölkopf, and A. Smola, "A kernel two-sample test," *Jrnl of Mach. Learning Res.*, vol. 13, no. 25, pp. 723–773, 2012.

[32] Y. Mao, D. Dueri, M. Szmuk, and B. Açıkmeşe, "Successive convexification of non-convex optimal control problems with state constraints," in *Proc IFAC World Congress*, vol. 50, no. 1, 2017, pp. 4063–4069.

[33] S. LaValle, *Planning Algorithms*. Cambridge Univ. Press, 2006.

[34] "Mobile robot kinematics equations," https://www.mathworks.com/help/robotics/ug/mobile-robot-kinematics-equations.html.

[35] A. Thorpe and M. Oishi, "SOCKS: A stochastic optimal control and reachability toolbox using kernel methods," in *Hybrid Systems: Computation and Control*, 2022.